Neuron, Vol. 24, 929–940, December, 1999, Copyright ©1999 by Cell Press

Human Cortical Regions Involved in Extracting Depth from Motion

Guy A. Orban,*§ Stefan Sunaert,† James T. Todd,‡ Paul Van Hecke,† and Guy Marchal†
*Katholieke Universiteit te Leuven
Faculty of Medicine
Laboratorium voor Neuro- en Psychofysiologie
†Universitair Ziekenhuis Gasthuisberg
Department of Radiology
Campus Gasthuisberg
B-3000 Leuven
Belgium
‡The Ohio State University
Department of Psychology
Columbus, Ohio 43210

Summary

We used functional magnetic resonance imaging (fMRI) to investigate brain regions involved in extracting three-dimensional structure from motion. A factorial design included two-dimensional and three-dimensional structures undergoing rigid and nonrigid motions. As predicted from monkey data, the human homolog of MT/V5 was significantly more active when subjects viewed three-dimensional (as opposed to two-dimensional) displays, irrespective of their rigidity. Human MT/V5+ (hMT/V5+) is part of a network with right hemisphere dominance involved in extracting depth from motion, including a lateral occipital region, five sites along the intraparietal sulcus (IPS), and two ventral occipital regions. Control experiments confirmed that this pattern of activation is most strongly correlated with perceived three-dimensional structure, in as much as it arises from motion and cannot be attributed to numerous two-dimensional image properties or to saliency.

Introduction

Motion is a powerful cue to depth (Wallach and O'Connell, 1953). After all, amblyopics, who have no stereopsis, see depth well enough to drive their cars or play squash. Little is known about the neuronal mechanisms underlying this perceptual ability. One recent study by Xiao et al. (1997) has shown that MT/V5 neurons in monkeys encode the direction of speed gradients that correspond to the tilt in depth of planar surfaces specified by motion (see also Bradley et al., 1998). In the present functional imaging experiment, we wanted to determine if the human homolog of MT/V5 (Zeki et al., 1991) also contributes to the extraction of depth from motion. One potential difficulty in addressing this issue is that functional imaging measures activity levels, whereas single cell recordings measure selectivity. Because the selectivity in MT/V5 is produced by inhibition arising from the antagonistic surround (Xiao et al., 1997), one can expect that many neurons will fail to respond to fronto–parallel surfaces but that at least some of these neurons will be driven by stimuli portraying surfaces tilted in depth. Hence, we predict higher activity levels in human MT/V5 (hMT/V5+) for three-dimensional stimuli than for two-dimensional stimuli, and this difference, if large enough, should appear in the functional magnetic resonance imaging (fMRI) signal.

Most previous research on the visual perception of three-dimensional structure from motion has been restricted primarily to computational analyses and psychophysical experiments on human observers. One obvious focus of this research is the perception of an object's structural characteristics, such as its surface curvature or its overall extension in depth (e.g., Rogers and Graham, 1979; Todd, 1984; Perotti et al., 1998). Of equal importance, however, is the perception of an object's transformational characteristics, such as whether it is undergoing translation, rotation, or some form of nonrigid deformation (e.g., Todd, 1982; Todd et al., 1988; Perotti et al., 1996). There are several lines of evidence to suggest that the perceptual analysis of these different attributes may involve separate mechanisms. For example, stimulus manipulations that can influence the perceived rigidity of an object often have no effect on perceived shape, and vice versa (see Todd, 1984; Liter and Braunstein, 1998; Perotti et al., 1998).

In light of these observations, we created displays for the present experiment so that the structural and transformational aspects of observers' perceptions could be varied independently. We used a 2×2 factorial design with structure (two-dimensional versus three-dimensional) and rigidity (rigid versus nonrigid) as the two main factors. Subjects were required to fixate a target on the screen while passively viewing the dynamic stimuli. This way, brain activity related to each of the perceptual impressions could be studied using a single set of stimuli. The stimuli employed in the present study were specifically adapted from previous psychophysical investigations of Todd (1982) and Perotti et al. (1996). Each display contained a random configuration of six connected line segments whose relative image trajectories were manipulated to create the four different categories of perceived structure and motion. As control conditions, we used the passive viewing of both static displays (Zeki et al., 1991) and flickering displays. It has been argued that flicker stimuli are the only valid controls for disentangling temporal change from spatio–temporal change (Braddick et al., 1997). However, if this were an accepted standard, it would exclude hMT/V5+ as a motion sensitive area, because just as monkey MT/V5 neurons (Lagae et al., 1994; Qian and Andersen, 1994), this area responds to flicker (Tootell et al., 1995; Van Oostende et al., 1997).

Another important methodological problem we needed to address in designing this experiment was to somehow distinguish the MR signal changes associated with the perception of three-dimensional structure or

§To whom correspondence should be addressed (e-mail: guy.orban@med.kuleuven.ac.be).

rigidity from those that might arise just from the presence of spatial variations in image velocity. There is a growing body of psychophysical and neurophysiological evidence to indicate that complex motion patterns are broken down by the visual system into several different functionally distinct components, such as curl, divergence, or deformation (Regan and Beverley, 1978; Saito et al., 1986; Duffy and Wurtz, 1991; Orban et al., 1992). Not all of these components are directly relevant, however, to the perceptual analysis of structure and rigidity (Koenderink and van Doorn, 1977; Koenderink, 1986). For example, variations in image velocity due to pure size change or two-dimensional rotation are completely independent of three-dimensional shape. Indeed, there have been several algorithms proposed in the literature that explicitly remove those components from the image velocity field in order to simplify the required computations for determining structure from motion (see Todd and Bressan, 1990; Koenderink and van Doorn, 1991). Because of the uniqueness of the properties of pure size change and two-dimensional rotation, they were used in the present experiment as control stimuli. This made it possible to separate MR responses to motion patterns that create the impression of depth or rigidity (e.g., as in Xiao et al., 1997) from MR responses that result from more general variations of image velocity.

Results

Main Experiment: Group Analysis

In our initial examination of the data, we averaged the activation patterns of all subjects to perform an omnibus group analysis. The primary advantage of this approach is that it allows inferences to be made about humans in general (Holmes and Friston, 1998), and not just the particular subjects tested. The two main effects of the factors, structure and rigidity, define four basic contrasts among the patterns of activation in the different conditions: rigid minus nonrigid, nonrigid minus rigid, three-dimensional minus two-dimensional, and two-dimensional minus three-dimensional. Among these four contrasts, the three-dimensional minus two-dimensional comparison was the only one to yield significant effects in the group analysis. There were eight separate regions for which the three-dimensional displays produced significantly more activation than did the two-dimensional displays. These are listed in Table 1, ranked in order of their level of significance. The MR signal changes listed in Table 1 are relatively small, <1%. This is largely due to the between subject averaging. Indeed, in the group analysis the average difference between three-dimensional and two-dimensional displays for right hMT/V5+ was 0.26% (Table 1), while in the single subject analyses the median value of this difference was 0.60%. The location of the eight regions within horizontal brain sections are highlighted in Figure 1. The most significant activation was in the region predicted by our monkey data: the right hMT/V5+ ("1" in the figure) in the ascending limb of the inferior temporal sulcus (ITS), as described earlier by Zeki et al. (1991), Watson et al. (1993), Tootell et al. (1995), and DeYoe et al. (1996). Our labeling of the other seven regions of increased activation is more tentative, and further work is needed to confirm whether or not they are functionally distinct.

Table 1. Group Analysis

Regions	Coordinates			% MR Signal Changes Compared with STA					Factorial Analysis (Z Score)[c]			3D − FLI	2D − STA
	x	y	z	3Dr	3Dnr	2Dr	2Dnr	FLI	3D − 2D[a]	NR − R[b]	Interaction	Z score	Z score
(1) Right hMT/V5+	52	−62	−4	0.59	0.67	0.29	0.43	0.61[e]	**6.27**[c]	3.11	ns	ns[d]	**6.65**[d]
(2) Right DIPSA	30	−38	72	0.32	0.33	0.08	0.24	0.11	**5.9**	3.45	2.89	**6.11**	**5.01**
(3) Right LOS	36	−82	6	0.34	0.29	0.02	0.14	0.41	**5.89**	ns	2.64	−2.28	2.08
(4) Left DIPSA	−34	−42	64	0.32	0.32	0.17	0.20	0.13	**5.32**	ns	ns	**6.02**	**5.87**
(5) Right POIPS	28	−76	38	0.45	0.51	0.23	0.28	0.40	**5.01**	ns	ns	ns	**4.73**
(6) Right TRIPS	30	−80	18	0.37	0.37	0.10	0.17	0.47	**4.91**	ns	ns	−1.9	2.55
(7) Left DIPSL	−32	−52	64	0.38	0.35	0.21	0.23	0.21	**4.90**	ns	ns	**4.38**	**5.7**
(8) Left TRIPS	−26	−82	14	0.27	0.24	0.09	0.12	0.37	**4.88**	ns	ns	−3.47	3.14
Left hMT/V5+	−52	−66	2	0.69	0.74	0.51	0.58	0.68	3.41	ns	ns	ns[c]	**7.08**[c]
Right FEF	22	−6	62	0.19	0.15	0.12	0.13	0.00	ns	ns	ns	**4.82**	3.88

[a] 3D: viewing three-dimensional rigid and non rigid displays; 2D: viewing two-dimensional rigid and non rigid display.
[b] NR: viewing non rigid three-dimensional and two-dimensional displays; R: viewing rigid three-dimensional and two-dimensional displays.
[c] Z scores are for activation height; those in bold are significant at $p_{corr} < 0.05$ for height and $p < 0.05$ for extent.
[d] Significance tested only in the eight regions yielded by three-dimensional minus two-dimensional.
[e] Replotting of data in Figure 2A.
ns: not significant at $p < 0.05$, uncorrected.

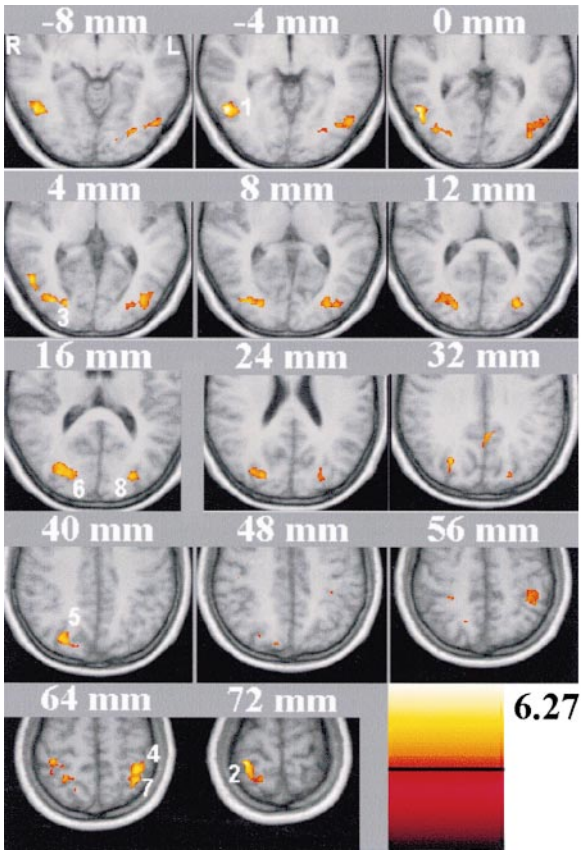

Figure 1. Group Analysis

SPMs showing the average difference between viewing of three-dimensional rigid and nonrigid displays and viewing of similar two-dimensional displays (three-dimensional minus two-dimensional). These regions are superimposed onto horizontal sections (right hemisphere on the left) through average MRI scans to show anatomical brain features. Horizontal sections range from 8 mm below to 72 mm above the anterior commissure–posterior commissure line. The color codes indicating level of significance ($z > 3.09$) are shown on the right. The eight sites significant in the three-dimensional–two-dimensional contrast are numbered 1 to 8. (1) right hMT/V5+, (2) right DIPSA, (3) right LOS, (4) left DIPSA, (5) right POIPS, (6) right TRIPS, (7) left DIPSL, and (8) left TRIPS (for coordinates, see Table 1).

Three of the activation sites were located in occipital cortex: one in the right lateral occipital sulcus (LOS; "3" in Figure 1), which is dorsal, posterior, and medial from hMT/V5+, and two bilateral regions at the most ventral end of the occipital extension of the intraparietal sulcus (IPS). Since these latter sites are located at the crossing of the intraparietal and transverse sulci, we tentatively labeled them TRIPS ("6" and "8" in Figure 1). They are located slightly more ventral to another region in the occipital extension of IPS that is responsive to motion and that has previously been labeled VIPS by Sunaert et al. (1999). That VIPS and TRIPS are distinct regions is underscored by the fact that TRIPS does not respond well to two-dimensional motion (see Table 1 and Figure 5). The label TRIPS has also been used by Culham et al. (1999) for a motion-responsive area that they tentatively identified as hV3A (Tootell et al., 1997). This latter area is located on the transverse sulcus, but more posteriorly than our TRIPS region. Thus, we feel it is justified to maintain our present nomenclature.

The four other sites with increased activation for three-dimensional stimuli are located dorsally in parietal cortex along the IPS and correspond to regions whose responsiveness to motion has been identified in our earlier investigations (Sunaert et al., 1999). One is located in the right hemisphere at the intersection of IPS and the parieto–occipital sulcus. This is referred to as POIPS ("5" in Figure 1). Two other sites, referred to as right and left DIPSA ("2" and "4" in Figure 1), are located dorsally in each hemisphere at the junction of IPS and the postcentral sulcus. Finally, in the left hemisphere, a region ("7" in Figure 1) along the dorsal IPS, just medial and posterior from left DIPSA, is also activated in the three-dimensional–two-dimensional contrast. It seems to correspond to DIPSL, another human motion-responsive area identified in Sunaert et al. (1999). It is interesting to note that activation of the parietal regions is smaller in magnitude than the activation that occurs in the occipital cortex (see Table 1), though they are comparable to one another in terms of their statistical significance. Because parietal regions are further removed from primary visual cortex, their visual signals are presumably weaker. Also, it should be stressed that the average coordinates of these sites are separated by more than 15 mm, thus suggesting, given the smoothness of the statistical parametric maps SPMs (see Experimental Procedures), that they might indeed be distinct functional regions. For that reason, we excluded from the list of sites one that just reached significance and might correspond to right hV3A but was too close (between 10 and 15 mm) to right LOS to be considered a separate region with some confidence.

Figure 2A plots the activity profile of right hMT/V5+, showing the adjusted MR signal for the six conditions: three-dimensional rigid, three-dimensional nonrigid, two-dimensional rigid, two-dimensional nonrigid, static, and flicker. The corresponding time courses for the group and a single subject are shown in Figure 2B. It is plain that the two three-dimensional conditions yield a stronger activation than the corresponding two two-dimensional conditions. There is also a hint that the two nonrigid conditions activate this region more than their rigid counterparts. Indeed, there was a weak trend in this direction in right hMT/V5+, as there was in right DIPSA (see Table 1). Furthermore, in right hMT/V5+ the difference in MR signal between three-dimensional and two-dimensional conditions was nearly the same for rigid and nonrigid displays. In general, the statistical analysis revealed no interaction between the two factors, although a relatively weak interaction was observed in right DIPSA and LOS (see Table 1).

In the left hemisphere, hMT/V5+ was more active in three-dimensional than in two-dimensional conditions, but the effect did not reach significance when corrected for multiple comparisons (Table 1). It exemplifies a number of motion-responsive regions that have a tendency to be more active in three-dimensional than two-dimensional conditions. Other examples were VIPS in both hemispheres and right postcentral region (Sunaert et al., 1999). On the other hand, right frontal eye field (FEF; Table 1) exemplifies those motion-responsive regions

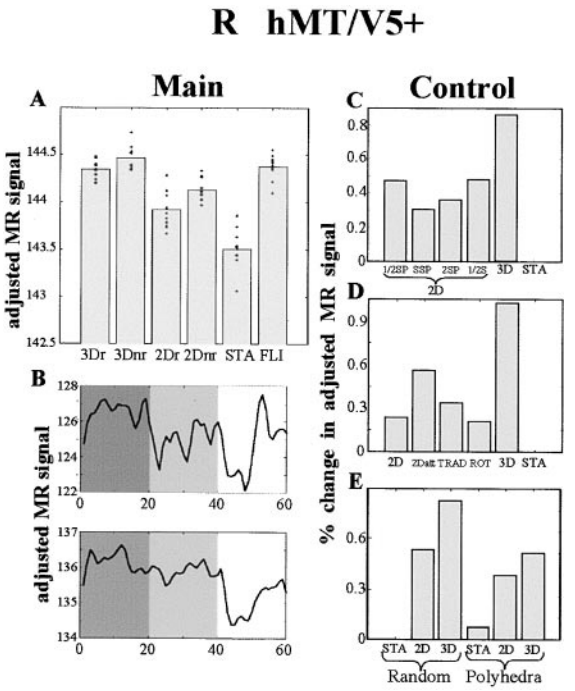

Figure 2. Group Analysis of Main and Control Experiments for Right hMT/V5+

(A) Activity profile of right hMT/V5+ obtained in the main experiment. Adjusted MR signal (resulting from proportional scaling), averaged over 11 subjects, is plotted for the six conditions of the main experiment: three-dimensional rigid (3Dr), three-dimensional nonrigid (3Dnr), two-dimensional rigid (2Dr), two-dimensional nonrigid (2Dnr), static (STA), and flickering (FLI) displays. The dots indicate individual responses. The profile is that of the most significant voxel, the coordinates of which are indicated in Table 1. Notice that in right hMT/V5+, the difference between three-dimensional rigid and two-dimensional nonrigid is still significant ($z = 3.01$).

(B) Time course of adjusted MR signal in right hMT/V5+ for one of the six time series of the main experiment: in a single subject (subject 10, average of 4 presentations) and in the group of 11 subjects (average of 44 presentations). The MR signal is plotted as a function of image number; each image corresponds to 3.5 s, for a total of 210 s. In this time series, the order of conditions is as in (A): dark hatching, three-dimensional conditions; light hatching, two-dimensional conditions; and no hatching, control conditions. The data in (A) result from averaging over the six time series, in which the order of conditions was changed.

(C–E) Activity profiles of right hMT/V5+, obtained in control experiment 1, rigid case (C); control experiment 2 (D); and control experiment 3 (E). The percent change in adjusted MR signal, relative to viewing static displays, averaged over two (C) or three (D and E) subjects, is plotted for the different conditions: two-dimensional rigid with half the standard speed (1/2SP), with standard speed (SSP), with double speed (2SP), and with half-size (1/2S); three-dimensional rigid and static in (C); two-dimensional rigid (2D), two-dimensional rigid with attention (2Datt), rotation in the fronto–parallel plane (ROT), trajectory-in-depth (TRAD), three-dimensional rigid (3D), and static (STA) in (D); and random lines, static in two-dimensional and three-dimensional motion and polyhedra, static in two-dimensional and three-dimensional motion in (E).

that are activated more or less equally by three-dimensional and two-dimensional conditions. Additional examples, all in left hemisphere, were FEF, postcentral region, POIPS, and DIPSM.

Table 1 also suggests that comparisons among the various control conditions might make it possible to discern finer distinctions among the eight different regions that were significantly activated by three-dimensional motion. Note in particular that right hMT/V5+ is significantly less responsive to static displays than to two-dimensional motion, which is hardly surprising, given that this is close to the original contrast for defining hMT/V5+ (Zeki et al., 1991). While right POIPS and the dorsal parietal regions respond to two-dimensional motion, right LOS and right and left TRIPS do not. Note also that the responsiveness of hMT/V5+ to three-dimensional conditions is not significantly different from that for flickering displays. This result is consistent with earlier comparisons of flicker and two-dimensional motion performed by Tootell et al. (1995) and Van Oostende et al. (1997). The three dorsal parietal regions, however, are also less responsive to flickering displays than to three-dimensional motion. This again fits with our earlier two-dimensional motion study (Sunaert et al., 1999).

Main Experiment: Single Subject Analysis

To complement our group analysis, a single subject analysis was also performed to provide maximal anatomical detail, to assess the variability across subjects, and to allow within-subject comparisons among the different conditions. Figure 3 shows a typical pattern of activation depicted in a sample of coronal sections and in surface views. In this particular subject, all significant activation sites were located in the right hemisphere, although some symmetrical regions were weakly activated in the left hemisphere. In examining this figure, it is possible to recognize four activation sites from the group analysis: hMT/V5+ ("a"), located along the ascending limb of the ITS; DIPSA ("e"), at the confluence of IPS and the postcentral sulcus; LOS ("b"), in the depth of the LOS; and TRIPS ("c"), at the most posterior end of the occipital extension of IPS, where it meets the transverse sulcus (see section "−80 mm"). Sites in single subjects were determined to be the same as those of the group analysis by three criteria: location with respect to anatomical landmarks (mainly sulci), Talairach coordinates, and relative position with respect to other activation sites. In this particular subject, two additional sites are located along the IPS. One ("d") is located in the middle of the dorso–ventral extent of the occipital part of IPS and corresponds to VIPS, as described by Sunaert et al. (1999). Finally, there was significant activation in the region corresponding to DIPSL ("f"), symmetrical to the left hemisphere site identified in the group analysis. Although activation extends continuously along the dorsal lips of IPS, the two sites DIPSA and DIPSL appear reasonably distinct. Similarly, LOS, TRIPS, and VIPS, which have relatively similar average coordinates, appear to be clearly separate sites in this subject. Indeed, along the cortical surface, LOS and TRIPS are actually quite far apart due to the fact that they are located in different sulci.

Because the group analysis reflects activation patterns of human subjects in general, one would expect the eight sites identified in the group analysis to be significant in the majority of the individual subjects. Indeed, all eight sites were significant in at least half the subjects, although there was some variation between

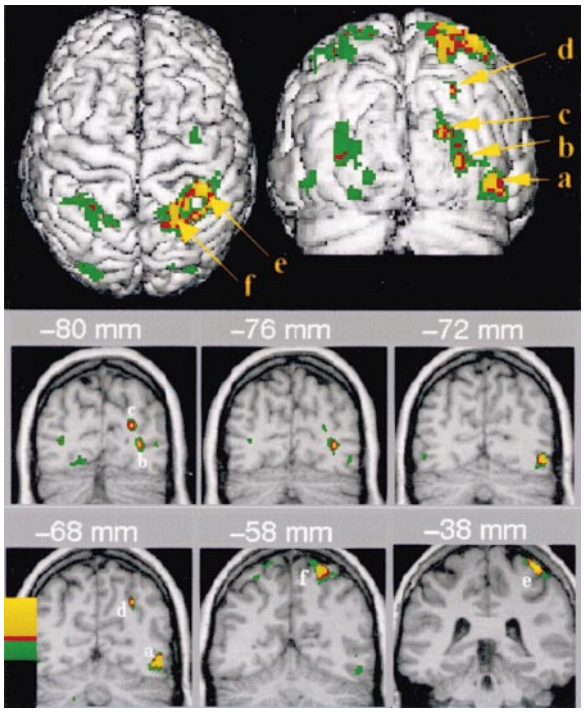

Figure 3. Single Subject Analysis

SPMs showing the difference between viewing of three-dimensional rigid and nonrigid displays and viewing of similar two-dimensional displays in subject 3. Voxels reaching different levels of activation (yellow: $p < 0.05$, corrected; red: $p < 0.2$, corrected; green: $p < 0.001$, uncorrected) are shown on superior and posterior views of the rendered brain (top) and on selected coronal sections (bottom). Maximum Z score was 7.19 in this subject. The letters indicate the six regions reaching statistical significance ($p < 0.05$, corrected): right hMT/V5+ (a), right LOS (b), right TRIPS (c), right VIPS (d), right DIPSA (e), and right DIPSL (f). Notice that symmetrical regions in the left hemisphere reached nonsignificant activation levels.

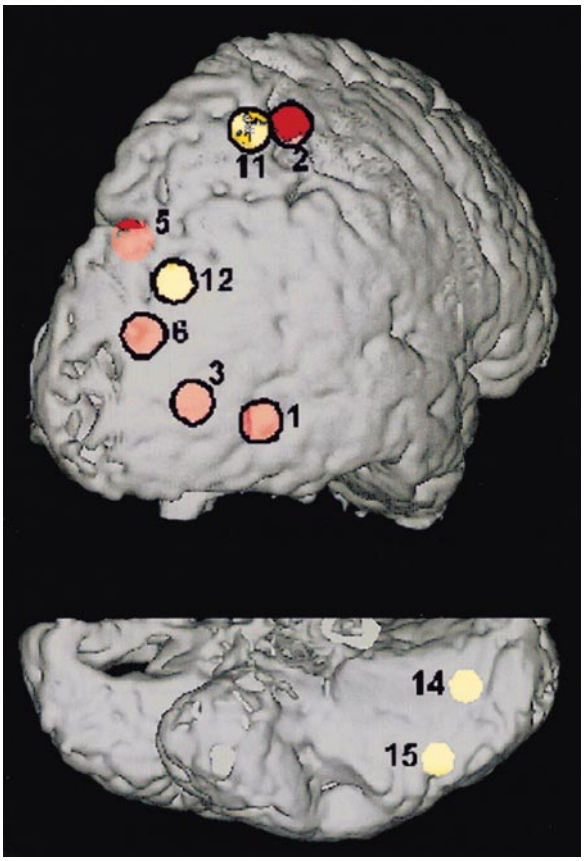

Figure 4. The Nodes of the Three-Dimensional Processing Network in the Right Hemisphere Shown on the Average Rendered Brain in Postero–Lateral and Inferior Views

Red: nodes yielded by group and single subject analysis; yellow: nodes yielded only by single subject analysis. The nodes with a black circle have a counterpart in the left hemisphere. The numbers 1 to 8 correspond to those in Table 1. (1) right hMT/V5+ (10/11 subjects; median coordinates: 51, −63, −5) and left hMT/V5+ (7/11; −50, −70, −2), (2) right DIPSA (8/11; 35, −42, 70) and left DIPSA (6/11; −41, −39, 62), (3) right LOS (8/11; 39, −77, 0) and left LOS (9/11; −36, −82, 2), (5) right POIPS (10/11; 18, −82, 41), (6) right TRIPS (11/11; 28, −86, 18) and left TRIPS (7/11; −28, −86, 16), (11) right DIPSL (7/11; 28, −50, 68) and left DIPSL (6/11; −31, −53, 64), (12) right VIPS (7/11; 30, −78, 32) and left VIPS (6/11; −25, −85, 29), (14) right collateral sulcus (8/11; 22, −75, −14), and (15) right fusiform cortex (7/11; 46, −66, −18).

the regions (Figure 4). Right hMT/V5+ was significant in 10 of 11 subjects. Furthermore, the median coordinates (see Figure 4) of the three-dimensional activation sites in individual subjects agree well with those of the group analysis (see Table 1). However, the single subject analysis also revealed seven additional regions that were significantly activated in 6 or more of the 11 subjects (see Figure 4). Three sites were symmetrical to regions identified by the group analysis: left hMT/V5+, left LOS, and right DIPSL. Others included VIPS (bilaterally), the right collateral sulcus, and the right fusiform gyrus. All of this suggests that the perception of three-dimensional (as opposed to two-dimensional) motion automatically activates a bilateral cortical network with right hemisphere dominance (see Figure 4) which includes two lateral occipital regions (hMT/V5+ and LOS), five regions following the IPS along its occipito–parietal extent (TRIPS, VIPS, POIPS, DIPSL, and DIPSA), and two ventral occipital regions (collateral sulcus and fusiform gyrus).

Up to now, we have identified the activation of hMT/V5+ in the three-dimensional–two-dimensional contrast on the basis of its location close to the ascending limb of the ITS. It is important to note that hMT/V5+ is a large region extending over more than 12 mm in all directions. Thus, it is necessary to ascertain whether the activation we observed in the three-dimensional–two-dimensional contrast corresponds to hMT/V5+ itself, a satellite region, or some other neighboring site. To address this issue, we attempted to localize hMT/V5+ in each subject independently by a contrast, comparing moving and stationary random textured patterns, that has traditionally been used to identify this area (Zeki et al., 1991; Dupont et al., 1994; Van Oostende et al., 1997). In each subject, we then measured the difference, in coordinates, between the most significant voxel of hMT/V5+ in the moving/stationary subtraction and the most significant voxel of the putative hMT/V5+ derived from the three-dimensional minus two-dimensional subtraction. The median ($n = 11$) signed differences in x, y, and z coordinates were −2, 0, and 4, and 4, 2, and 4 mm

for right and left hMT/V5+, respectively. Thus, we can safely conclude that three-dimensional displays, compared with two-dimensional displays, activate hMT/V5+ proper. To test for the significance of the interhemispheric difference in hMT/V5+ activation, we compared three-dimensional evoked activity in the two hemispheres after additional smoothing (smoothness estimate, 15 mm) to overcome possible anatomical differences. Restricting the test to the independent voxels (Worsley et al., 1996) of hMT/V5+ yielded a significant difference ($z = 3.8$, $p_{corr} < 0.05$).

Control Experiment 1

In creating the motion displays for the four experimental conditions of the main experiment, we attempted to equate the average values of two basic image parameters: the length of line segments and the speed of translation of their endpoints. A posteriori computation of the median values across all frames and displays showed that the speeds ranged from 2.23° to 2.99° per second and that the lengths varied from 5.62° to 6.45° (Table 3). To exclude the possibility that these small variations in image characteristics could account for MR signal differences between the experimental conditions, we ran a control experiment in which three-dimensional motions were compared with four distinct two-dimensional conditions: one with standard size and speed, one with the speed halved, one with the speed doubled, and one with the size halved. Viewing of static displays was added as a reference condition. We ran this control in two subjects with rigid displays and two others with nonrigid displays. As shown in Table 2, all two-dimensional conditions produced MR signals of about the same strength, and they were all significantly smaller than those produced by the three-dimensional conditions. This was the case for right hMT/V5+, in both the rigid (Figure 2C) and nonrigid cases, and for other nodes of the three-dimensional processing network, except left DIPSA. It should be noted that the variation in speed and size in these control experiments far exceeds the average differences between three-dimensional and two-dimensional conditions in the main experiment. The lines in the three-dimensional displays moved on average only 30% faster and were 15% shorter than in the two-dimensional displays.

Control Experiment 2

There are, however, several other higher order attributes of the moving displays that were not equated across the four main experimental conditions. These include dynamic changes in length or orientation of the different line segments and the instantaneous variations in the velocities of their endpoints. To evaluate the importance of these variables, we designed two additional control conditions. To create variations in line orientation and the instantaneous pattern of endpoint velocities, we used a pure rotation in the fronto–parallel plane. We also combined a size change transformation with translation in the fronto–parallel plane, which created the impression of a planar object, parallel to the fronto–parallel plane, orbiting along a circular trajectory in depth. In the three-dimensional conditions of the main experiment, the line segment endpoints appeared to oscillate in depth, and the question arises whether neural activation is due to the perceived three-dimensional structure of the object or the three-dimensional trajectories of its endpoints. A final condition controlled for differences in attention that the subjects may have devoted to the two-dimensional and three-dimensional motion patterns. It could be argued that the three-dimensional displays are more salient, and that variations in neural activation are due solely to changes in attention. To test this hypothesis, we adopted a procedure of Buchel et al. (1998) to manipulate the salience of two-dimensional motion displays. In this two-dimensional attention condition, the stimulus was identical to the two-dimensional condition, but subjects looked for transient speed changes.

The results of these control experiments ($n = 3$) are straightforward: both the rotation and trajectory-in-depth conditions evoked about the same level of MR signal as the standard two-dimensional rigid condition (Table 2). The two-dimensional attention manipulation increased MR signals in the three-dimensional network sites that reached significance in the three-dimensional minus two-dimensional subtraction of this experiment, and in particular in right hMT/V5+ (Figure 2D), yet these regions were all significantly less responsive in the two-dimensional attention condition than in the three-dimensional motion condition.

Control Experiment 3

In the three-dimensional conditions, the extraction of structure from motion is confounded with the simple combination of a three-dimensional structure and motion. Therefore, we designed a another control experiment, in which objects that appeared three-dimensional from static cues (rectangular polyhedra) were either translating in the fronto–parallel plane or rotating in depth. These conditions were compared with others similar to the main experiment, in which random line objects (random conditions) made of the same line segments as the polyhedra were perceived as two-dimensional or three-dimensional solely because of their motion.

The results of this factorially designed experiment ($n = 3$) were again straightforward. The three-dimensional motion random condition compared with the two-dimensional motion random condition activated three of the eight core three-dimensional network sites: right hMT/V5+, right LOS, and left TRIPS (Table 2). In all of these regions, the activity evoked by the three-dimensional motion random condition significantly exceeded that evoked by the polyhedra in two-dimensional motion (Table 2), as illustrated for right hMT/V5+ in Figure 2E. It is noteworthy that in this control experiment, as in control experiment 2, the three-dimensional–two-dimensional motion difference for random lines was not significant in left hMT/V5+. Probing the most significant voxels of right and left hMT/V5+ yielded by the control moving/stationary subtraction, the z scores for the three-dimensional–two-dimensional motion contrast in the random conditions were 7.23 and 3.1, respectively.

Discussion

As predicted from monkey results (Xiao et al., 1997; Bradley et al., 1998), the present experiment provides

Table 2. Group Analysis of Control Experiments

Regions	Coordinates			Z Score	% Change in Adjusted MR Signal, Relative to STA						Z Score Control Subtractions		
					Control Experiment 1 (Rigid Case, n = 2)								
	x	y	z	3D−2D SSP	2D 1/2SP	2D SSP	2D 2SP	2D 1/2S	3D	STA[a]	3D−2D 1/2SP	3D−2D 2SP	3D−2D 1/2S
(1) Right hMT/V5+	48	−60	−8	7.43	0.47%	0.31%	0.36%	0.48%	0.87%	0.00%	5.30	6.61	5.15
(2) Right POIPS	12	−84	44	7.09	0.29%	0.37%	0.45%	0.11%	1.11%	0.00%	8.27	6.47	9.27
(3) Right DIPSA	44	−36	64	6.57	0.35%	0.26%	0.33%	0.33%	0.70%	0.00%	5.13	5.47	5.24
(4) Right LOS	36	−84	−4	5.51	−0.02%	−0.03%	0.06%	0.13%	0.35%	0.00%	5.28	4.14	3.34
(5) Left DIPSA	−40	−32	68	4.97	0.01%	−0.08%	0.09%	−0.10%	0.18%	0.00%	3.38	1.63	1.67
					Control Experiment 1 (Non rigid Case, n = 2)								
	x	y	z	3D−2D SSP	2D 1/2SP	2D SSP	2D 2SP	2D 1/2S	3D	STA	3D−2D 1/2SP	3D−2D 2SP	3D−2D 1/2S
(6) Right hMT/V5+	48	−60	−4	5.88	0.32%	0.22%	0.36%	0.21%	0.57%	0.00%	4.43	3.65	6.60
(7) Right DIPSA	28	−40	72	5.2	0.44%	0.36%	0.46%	0.33%	0.70%	0.00%	4.08	4.05	5.73
					Control Experiment 2 (n = 3)								
	x	y	z	3D−2D	2D	2Datt	TRAD	ROT	3D	STA[b]	3D−2Datt	3D−TRAD	3D−ROT
(8) Right hMT/V5+	54	−69	−6	8.5	0.23%	0.54%	0.32%	0.20%	1.00%	0.00%	6.71	8.26	8.63
(9) Right TRIPS	30	−87	12	8.4	0.07%	0.24%	0.04%	−0.17%	0.54%	0.00%	7.55	8.53	8.90
(10) Left DIPSA	−36	−39	63	8.04	0.59%	0.74%	0.65%	0.24%	0.99%	0.00%	6.12	7.10	8.78
(11) Right DIPSA	33	−48	60	7.92	0.20%	0.34%	0.24%	0.05%	0.50%	0.00%	5.14	7.57	8.75
					Control Experiment 3 (n = 3)								
	x	y	z	Rand3D−Rand2D	RandSTA	Rand2D	Rand3D	PolySTA	Poly2D	Poly3D[c]	Rand3D−Poly2D		
(12) Right hMT/V5+	54	−60	0	7.36	0.00%	0.51%	0.82%	0.08%	0.38%	0.54%	8.13		
(13) Right LOS	39	−78	9	6.94	0.00%	0.19%	0.49%	0.02%	0.10%	0.28%	7.77		
(14) Left TRIPS	−30	−84	12	6.03	0.00%	0.11%	0.42%	0.00%	0.23%	0.38%	5.20		

[a] 2D 1/2SP, 2D SSP, 2D 2SP, and 2D 1/2S: two-dimensional conditions with speed halved, with standard speed, with speed doubled, and with size halved.
[b] 2Datt: two-dimensional with attention; TRAD: trajectory-in-depth; and ROT: rotation (in the fronto–parallel plane).
[c] Rand: random lines; and Poly: polyhedra.

strong evidence that the human homolog of MT/V5 responds more actively to three-dimensional motion than to two-dimensional motion. To confirm independently that the site of this three-dimensional activation was indeed hMT/V5+, we also performed a more traditional comparison between moving and stationary displays. Several additional controls were employed as well to test for the possibility that the increased activation of hMT/V5+ might not be due to the perception of depth per se, but to differences in stimulus characteristics, including higher order ones, such as changes over time in the lengths or orientations of the moving line segments. Further controls indicated that the critical element in the perception was the extension in depth of the figure induced by its motion, not just the motion in depth of the endpoints or the simple combination of depth in the figure with its motion.

It has been suggested (DeYoe et al., 1996) that hMT/V5+ is not just the homolog of MT/V5 but also of its satellites MST (medial superior temporal area) and FST (visual area in the fundus of the superior temporal sulcus) (hence the plus sign in the label). The results of Duffy and Wurtz (1997) suggest that MST neurons also process speed distributions that might signal three-dimensional structure. Thus, our results are in agreement with monkey physiological studies. They also agree with human lesion data (Vaina et al., 1990; Rizzo et al., 1995) and with a preliminary report on lesion effects in the monkey (R. M. Siegel and R. A. Andersen, 1986, Soc. Neurosci., abstract).

In our experiments, the activation of hMT/V5+ was asymmetrical. In the main experiment right hMT/V5+ was significantly more active in the three-dimensional conditions than its left counterpart. And indeed, in the group analysis, right hMT/V5+ was the most significant activation site in the three-dimensional minus two-dimensional subtraction, while left hMT/V5+ did not reach the corrected $p < 0.05$ threshold. Furthermore, in the single subject analysis, left hMT/V5+ was significantly activated in fewer subjects than its right counterpart. This asymmetry was confirmed in the second and third control experiments, the latter one using slightly different random line stimuli.

Another important finding of this study is that hMT/V5+ is not the only area activated by the three-dimensional–two-dimensional motion contrast. Rather, hMT/V5+ appears to be part of a larger cortical network involved in the processing of three-dimensional structure from motion. In addition to hMT/V5+, the network includes a region in the LOS, five regions along the IPS, a collateral sulcus site, and a region in the fusiform gyrus. The core regions of this network were all revealed by the group analysis, which is valid for humans in general. The remaining regions were significant in a majority of the individual subjects. Many of these regions have been shown to respond to moving stimuli either in passive conditions (Dupont et al., 1994; Dieterich et al., 1998; Goebel et al., 1998; Sunaert et al., 1999) or in active conditions (Cornette et al., 1998; Culham et al., 1998). It is important to keep in mind that the cortical network involved in processing three-dimensional structure from motion is only a portion of a more general motion-processing network (Sunaert et al., 1999). For example, one region that is clearly implicated in motion processing but not in structure from motion is the FEF. This is not surprising, since only two-dimensional information is needed to control saccades and pursuit, which are known to activate this premotor region (Petit et al., 1997). On the other hand, the dorsal parietal regions involved in extracting three-dimensional structure from motion can also be activated by static stimuli, such as those used in orientation discrimination (Cornette et al., 1999; I. Faillenot et al., 1999, Soc. Neurosci., abstract) or conjunction search (Corbetta et al., 1995; Leonards et al., 1999). Furthermore, areas along the dorsal IPS are also activated by eye movement and attention shifts (Corbetta et al., 1998).

Much like the response patterns in hMT/V5+, the depth-from-motion network is bilateral, but with a greater level of activity in the right hemisphere. It is interesting to note that this lateralized pattern of activation is consistent with a previous report by Vaina et al. (1996), who studied a stroke patient, subject RA, with a unilateral lesion in the right hemisphere. Subject RA was significantly impaired at judging three-dimensional structure from motion in both the right and left visual fields, but his judgments of heading direction from optical flow were normal. Based on the imaging and patient data, it would be reasonable to expect behavioral asymmetries in the perception of depth from motion, such that moving objects in the left visual field might be easier to judge than those on the right.

We have purposely employed descriptive names to label the different activation sites in this study in order to avoid making premature assumptions about homologies with known brain regions in monkeys. Despite the fact that several of these sites seem to correspond to those observed in earlier studies, as the labels indicate, we do not wish to imply that all of the designated regions are functionally distinct from one another. This remains open to further study.

It is important to keep in mind that the subjects in this study were tested under conditions of passive fixation. Thus, the network reported here as involved in the processing of three-dimensional structure from motion might well be one that processes these stimuli automatically. This might explain the preponderance of dorsal visual regions, which are known to be involved in visuo–motor control (Mountcastle et al., 1975). Indeed, it is likely that much of the automatic processing is geared toward reacting to visual inputs as quickly and precisely as possible. Clearly, the three-dimensional structure of objects is critical when grasping them, as is the three-dimensional structure of the surroundings in which one has to move around. We might therefore expect a number of regions to be more active when this additional information has to be processed. It is likely to be the case, moreover, that perceptual distinctions between rigid and nonrigid motion are equally important for visuo–motor control, and this could potentially explain the relatively weak effect of this manipulation under the present experimental conditions. Our previous research has shown that cerebral networks for automatic processing are modulated considerably by task requirements (Orban et al., 1997, 1998; Cornette et al., 1998). Perhaps this is also true for the network processing

three-dimensional structure from motion, and an exploration of that issue will set the agenda for our future experiments.

Experimental Procedures

The MR scans were performed on 20 right-handed subjects whose ages ranged between 18 and 29 years. They all had normal or corrected to normal vision and no history of neurological or psychiatric disease. The study was approved by the Ethical Committee of the KULeuven Medical School, and subjects gave their informed consent, in accordance with the Helsinki Declaration. All subjects wore an eye patch over the nondominant eye to eliminate conflicting three-dimensional information from binocular vision, and their head movements were immobilized using a bite-bar. They were instructed to maintain fixation on a small red target in the center of the screen and to perform no task other than fixation while passively viewing the stimuli. Subjects were familiarized with this task during an initial training session. Fixation was monitored using an MR-compatible infrared eye movement tracking device (Ober 2, Permobil Meditech AB, Timrà, Sweden). An analysis of these recordings revealed that subjects made relatively few saccades (fewer than three per 35 s epoch) and that there were no significant differences among the various treatment and control conditions.

Stimuli were projected by means of a liquid crystal display projector (Sharp GX-3800, 640 $\times$ 480 pixels, 60 Hz refresh) onto a translucent screen positioned in the bore of the magnet at a distance of 30 cm from the point of observation. Stimuli were generated with a PC using a Tiga-diamond (Salient AT3000) graphics card. In all experiments except control experiment 3, each display contained a random configuration of six connected line segments, with its motion centered on the fixation point and a mean eccentricity of 4.5° (range, 0° to 13°).

The four main conditions were organized in a 2 $\times$ 2 factorial design with two levels of rigidity (rigid and nonrigid) and two levels of structure (two-dimensional and three-dimensional). Some representative trajectory patterns for these different conditions are shown in Figure 5. For the three-dimensional rigid displays, the endpoints of each line segment oscillated back and forth in a horizontal direction around the center of the display screen. All endpoints oscillated with the same frequency, although their amplitudes and phases were varied independently of each other. A similar pattern was used for the two-dimensional rigid displays, except that all of the moving endpoints had an identical phase and amplitude. For the three-dimensional nonrigid displays, all of the oscillation parameters (direction, frequency, amplitude, and phase) were selected at random for each endpoint. Finally, in the two-dimensional nonrigid condition, the configurations were subjected to an oscillatory shear transformation. Although this transformation has a possible three-dimensional rigid interpretation as a planar surface slanted in depth, it appears perceptually as a nonrigid two-dimensional transformation whenever the magnitude of the shear is sufficiently large. In all four conditions, a rotation in the image plane was added to eliminate direction as a confounding cue. (Note, however, that this rotation has been excluded from the trajectories shown in Figure 5 so as not to mask the systematic differences among the various conditions.) The control conditions in the main experiment included a static condition, in which a random configuration of line segments remained stationary, and a flicker condition, in which a new configuration was presented every ten frames.

A large number of displays for each condition were created at random, subject to the constraints described above. Prior to their inclusion in the final stimulus set, however, they were screened by three observers to reject any configurations whose apparent rigidity or dimensionality were perceptually ambiguous or did not conform to the intended category. Based on this screening, a set of 19 displays was selected for each condition to be used in the actual experiment. During a debriefing session immediately following the MR scan, all subjects acknowledged that they had experienced the intended perceptual impressions.

In designing these displays, we wanted to ensure that any differences in brain activity they evoked would be due to the intended perceptual classifications and not to differences in their two-dimensional image properties. Thus, we attempted to adjust the display parameters so that the different conditions would all be approximately matched in terms of several different statistical measures. These included the average line length, the average change in line length and orientation at each frame transition, the average image displacement of the line segment endpoints, and the standard deviations of those displacements in the horizontal and vertical directions. To eliminate changes in angle or the directions of motion as potential cues for distinguishing the different conditions, a two-dimensional image rotation was added to each of the four basic categories of motion shown in Figure 5. We also included a number of additional variations of the two-dimensional rigid displays to manipulate a variety of image parameters, independent of the main factors of rigidity and dimensionality. These included displays moving at half or twice the speed as in the main condition; displays that were only half as big as in the main condition; displays undergoing pure rotation in the fronto–parallel plane (rigid rotation in Figure 5), so that their endpoints would exhibit large variations in image velocity; and displays with an oscillatory scaling transformation, so that the lengths of the line segments would change over time (size change in Figure 5). This latter type of display appears perceptually as a

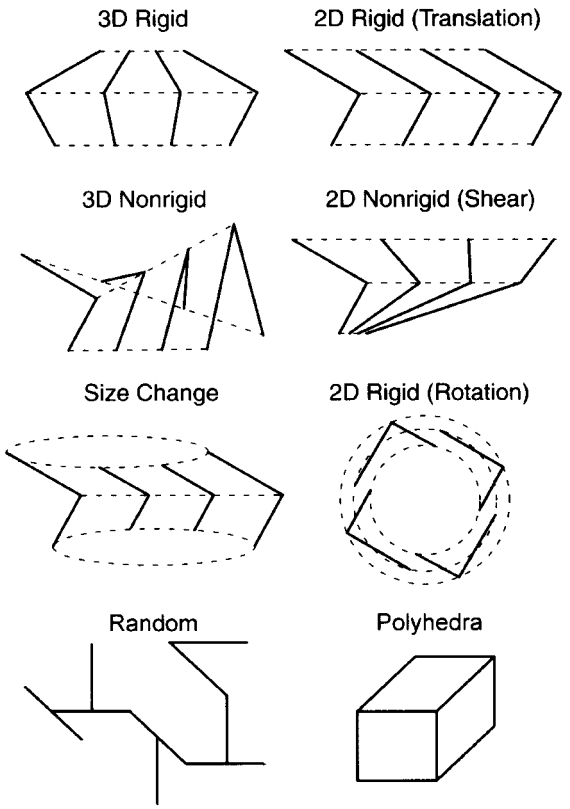

Figure 5. Six Possible Patterns of Motion and Two Types of Objects that Were Used in the Present Experiment

In the upper panels, the solid lines in each figure depict the image projections of pairs of line segments at four distinct moments in time, and the dotted lines represent the space–time trajectories of their endpoints. Note that in our three-dimensional displays, the oscillatory movements of the line segment endpoints had randomly independent phases, while those in the figure all have the same phase to prevent the different temporal snapshots from spatially overlapping one another. The size change appears as a flat object traveling in depth (trajectory-in-depth condition).

The top four motion patterns were used in the main experiment and in control experiment 1, size change and rigid rotation were used in control experiment 2, and the two types of objects were compared in control experiment 3.

flat two-dimensional figure that moves back and forth in depth as it oscillates in the display screen and is labeled TRAD in Figure 2. The statistical measures for these various conditions are provided in Table 3. While all stimuli in the main experiment and the two first control experiments were random lines, we explicitly compared rectangular polyhedra and corresponding random line objects in the last control experiment (Figure 5). Since the random lines contained the same line segments as the polyhedra, there were nine connected line segments, which, when appearing three-dimensional, formed rectangular angles, rather than six segments that made arbitrary angles in three dimensions. Other stimulus parameters such as length, speed, and eccentricity were very similar to those in the initial experiments.

A functional imaging series consisted of 120 gradient-echo echoplanar imaging whole brain scans (Siemens Vision 1.5T) acquired every 3.5 s (time of echo, 40 ms; flip angle, 90°; 64 × 64 matrix; 200 × 200 mm² FOV; 32 noncontiguous slices; 4 mm slice thickness; 1 mm gap). Within one time series, six conditions, each presented twice for 35 s (10 images), alternated in random order, yielding 20 images per condition. These series were repeated 12 times in two sessions, with the conditions in different order, yielding 240 images per condition, except in the third control experiment, in which they were repeated 6 times. One functional series included the six conditions of the main experiment (2 × 2 factorial plus two controls). For each repetition of this series, 2 displays of each type were selected randomly from the set of 19 generated. A second series corresponded to the first control experiment and included three-dimensional and two-dimensional conditions of one type (either rigid or nonrigid) and the static condition. The two-dimensional conditions were standard, with speed either halved or doubled or with size halved. The third series corresponded to the second control experiment. It included the two-dimensional rigid, three-dimensional rigid, static, pure rotation and trajectory-in-depth conditions. In a final sixth condition, the stimulus was a two-dimensional rigid display, but the subject looked for transient changes in speed (Buchel et al., 1998). Afterward, the subjects were asked whether they perceived changes, although none were present. Subjects reported to have seen between two and six changes. In preliminary sessions, the subjects had seen two-dimensional rigid displays in which speed effectively changed briefly, but the size of the speed change was gradually reduced over the runs. The fourth series corresponded to the third control experiment: the factorial design with object type (two levels: polyhedra and random lines) and motion pattern (three levels: static, translation, and rotation in depth) yielded six conditions. In each subject, we also used a functional series in which only two conditions, moving random textured patterns and the same patterns stationary, alternated, as described in Van Oostende et al. (1997). Only 120 images were sampled for these conditions. This series was used to localize hMT/V5+ in each subject (Dupont et al., 1994; Van Oostende et al., 1997). Sagittal anatomical images were acquired before the functional scanning in each session (three-dimensional magnetization-prepared rapid acquisition gradient echo, time of recovery/time of echo = 11.4/4.4 ms, time of inversion = 300 ms, FOV 256 × 256 mm², 256 × 256 matrix, 160 mm slab thickness, 128 sagittal partitions).

Brain images were transferred to a work station (Silicon Graphics), corrected for motion, coregistered with anatomical images, normalized to Talairach space, and smoothed (isotropic Gaussian kernel, 5 mm and 8 mm half-width at half-maximum) for single and group analysis, repetition (Friston et al., 1995). SPMs were computed using SPM96 (Friston et al., 1994a, 1994b). Analysis was restricted to regions behind the anterior commissure. The different conditions were modeled with a box car function convolved with the hemodynamic response function implemented as a delayed Gaussian function (Friston et al., 1995) in the context of the general linear model, as employed by SPM96. Global changes were adjusted by proportional scaling, and low-frequency confounding effects were removed by an appropriate high-pass filter. Specific effects were tested by applying appropriate linear contrasts to the parameter estimates for each condition, resulting in a t statistic for each and every voxel. These t statistics constitute an SPM. Both single subject and random effects (Holmes and Friston, 1998) group analysis, allowing population inference, were performed on the data of the main experiment. The different contrasts corresponding to the two main effects and their

Table 3. Image Characteristics of the Different Dynamic Conditions in Main Experiment and Control Experiments 1 and 2

		3Dr	3Dnr	2Dr	2Dnr	2Dr 1/2 spd	2Dr 2 spd	2 Dr 1/2 size	Rotation	Trajectory-in-depth
Length (degrees)	x	3.49 (2.62)[a]	3.96 (3.04)	3.87 (2.76)	4.09 (3.31)	3.97 (2.84)	3.59 (2.48)	1.74 (1.5)	4.04 (2.93)	3.28 (2.63)
	y	3.69 (2.68)	4.19 (3.16)	3.41 (2.77)	3.63 (2.97)	3.86 (2.96)	3.81 (2.78)	1.83 (1.36)	4.17 (3.04)	3.80 (2.90)
	Total	5.62 (2.88)	6.45 (3.30)	5.73 (3.00)	6.09 (3.55)	6.14 (3.13)	5.80 (2.77)	2.81 (1.61)	6.44 (3.17)	5.52 (3.17)
Δ length (degrees/s)	x	1.79 (1.56)	2.13 (1.81)	0.41 (0.33)	1.63 (1.84)	0.46 (0.35)	0.46 (0.33)	0.22 (0.16)	2.50 (1.82)	0.47 (0.40)
	y	1.90 (1.80)	2.38 (1.88)	0.46 (0.33)	1.66 (1.78)	0.48 (0.34)	0.43 (0.29)	0.21 (0.18)	2.41 (1.76)	0.47 (0.41)
	Total	1.37 (1.56)	2.29 (1.79)	0 (0)	1.24 (1.16)	0 (0)	0 (0)	0 (0)	0 (0)	0.54 (0.45)
Speed (degrees/s)	x	1.43 (1.15)	1.42 (1.36)	1.87 (1.36)	1.66 (1.31)	1.07 (0.74)	4.31 (2.80)	1.76 (1.32)	1.75 (1.11)	2.13 (1.06)
	y	1.46 (0.02)	1.48 (0.02)	1.92 (0.02)	1.76 (0.02)	1.05 (0.01)	3.21 (0.04)	2.02 (0.02)	1.69 (0.02)	0.93 (0.01)
	Total	2.23 (0.02)	2.29 (0.03)	2.99 (0.02)	2.64 (0.03)	1.67 (0.01)	5.93 (0.05)	2.97 (0.02)	2.70 (0.02)	2.43 (0.01)
Δ angle (degrees/s)		33.42 (65.5)	30.46 (72.3)	6.88 (0)	18.38 (15.4)	6.88 (0)	6.88 (0)	6.88 (0)	34.38 (0)	4.81 (0.00)
Standard deviation of speed (degrees/s)	x	1.48 (0.68)	1.75 (0.55)	0.32 (0.12)	1.34 (1.0)	0.36 (0.11)	0.35 (1.0)	0.17 (0.05)	1.89 (0.58)	0.36 (0.17)
	y	1.54 (0.83)	1.84 (0.67)	0.36 (0.08)	1.33 (0.93)	0.36 (0.11)	0.32 (1.0)	0.17 (0.05)	1.81 (0.56)	0.36 (0.17)

[a] Mean and (standard deviation) of image quantities.

interaction were tested. The control experiments were analyzed in a fixed-effect group analysis, and only the subtraction three-dimensional minus two-dimensional was used to define the different regions activated by three-dimensional motion. In Table 2, we restricted the analysis to those of the eight core regions, significant in the group analysis of the main experiment, that reached significance in the three-dimensional minus two-dimensional subtraction of a given control experiment. The activity in the most significant voxel of these regions was then compared in the different conditions. Results were very similar when we also included in the analysis the nodes of the three-dimensional structure-from-motion processing network that were significant in at least half of the single subjects. The smoothness of the SPMs was 7 and 9 mm for the single subject and group analysis, respectively. Significance thresholds were set at $p < 0.05$, corrected for multiple comparisons for activation height, and at $p < 0.05$ for activation extent.

Received April 2, 1999; revised October 6, 1999.

References

Braddick, O.J., Hartley, T., Atkinson, J., Watton-Bell, J., and Turner, R. (1997). fMRI study of differential activation by coherent motion and dynamic noise. Invest. Ophthalmol. Vis. Sci. *38*, S919.

Bradley, D.C., Chang, G.C., and Andersen, R.A. (1998). Encoding of three-dimensional structure-from-motion by primate area MT neurons. Nature *392*, 714–717.

Buchel, C., Josephs, O., Rees, G., Turner, R., Frith, C.D., and Friston, K.J. (1998). The functional anatomy of attention to visual motion. A functional MRI study. Brain *121*, 1281–1294.

Corbetta, M., Shulman, G.L., Miezin, F.M., and Petersen, S.E. (1995). Superior parietal cortex activation during spatial attention shifts and visual feature conjunction. Science *270*, 802–805.

Corbetta, M., Akbudak, E., Conturo, T.R., Snyder, A.Z., Ollinger, J.M., Drury, H.A., Linenweber, M.R., Petersen, S.E., Raichle, M.E., Van Essen, D.C., and Shulman, G.L. (1998). A common network of functional areas for attention and eye movements. Neuron *21*, 761–773.

Cornette, L., Dupont, P., Rosier, A., Sunaert, S., Van Hecke, P., Michiels, J., Mortelmans, L., and Orban, G.A. (1998). Human brain regions involved in direction discrimination. J. Neurophysiol. *79*, 2749–2765.

Cornette, L., Dupont, P., Peuskens, H., Bormans, G., Claeys, K., De Schutter, E., Mortelmans, L., and Orban, G.A. (1999). Rate dependence of task-related cerebral activations: a PET-study. Neuroimage *9*, S856.

Culham, J.C., Brandt, S.A., Cavanagh, P., Kanwisher, N.G., Dale, A.M., and Tootell, R.B.H. (1998). Cortical fMRI activation produced by attentive tracking of moving targets. J. Neurophysiol. *80*, 2657–2670.

Culham, J.C., Dukelow, S.P., Vilis, T., Hassard, F.A., Gati, J.S., Menon, R.S., and Goodale, M.A. (1999). Recovery of fMRI activation in motion area MT following storage of the motion aftereffect. J. Neurophysiol. *81*, 388–393.

DeYoe, E.A., Carman, G.J., Bandettini, P., Glickman, S., Wieser, J., Cox, R., Miller, D., and Neitz, J. (1996). Mapping striate and extrastriate visual areas in human cerebral cortex. Proc. Natl. Acad. Sci. USA *93*, 2382–2386.

Dieterich, M., Bucher, S.F., Seelos, K.C., and Brandt, T. (1998). Horizontal or vertical optokinetic stimulation activates visual motion-sensitive, ocular motor and vestibular cortex areas with right hemispheric dominance. An fMRI study. Brain *121*, 1479–1495.

Duffy, C.J., and Wurtz, R.H. (1991). Sensitivity of MST neurons to optic flow stimuli. I. A continuum of response selectivity to large-field stimuli. J. Neurophysiol. *65*, 1329–1345.

Duffy, C.J., and Wurtz, R.H. (1997). Medial superior temporal area neurons respond to speed patterns in optic flow. J. Neurosci. *17*, 2839–2851.

Dupont, P., Orban, G.A., De Bruyn, B., Verbruggen, A., and Mortelmans, L. (1994). Many areas in the human brain respond to visual motion. J. Neurophysiol. *72*, 1420–1424.

Friston, K.J., Jezzard, P., and Turner, R. (1994a). Analysis of functional MRI time-series. Hum. Brain Map. *1*, 153–171.

Friston, K.J., Worsley, K.J., Frackowiak, R.S.J., Mazziotta, J.C., and Evans, A.C. (1994b). Assessing the significance of focal activations using their spatial extent. Hum. Brain Map. *1*, 214–220.

Friston, K.J., Holmes, A.P., Poline, J.B., Grasby, P.J., Williams, S.C.R., Frackowiak, R.S.J., and Turner, J. (1995). Analysis of fMRI time series revisited. Neuroimage *2*, 45–53.

Goebel, R., Khorram-Sefat, D., Muckli, L., Hacker, H., and Singer, W. (1998). The constructive nature of vision: direct evidence from functional magnetic resonance imaging studies of apparent motion and motion imagery. Eur. J. Neurosci. *10*, 1563–1573.

Holmes, A.P., and Friston, K.J. (1998). Generalisability, random effects and population inference. Neuroimage *7*, S754.

Koenderink, J.J. (1986). Optic flow. Vision Res. *26*, 161–179.

Koenderink, J.J., and van Doorn, A.J. (1977). How an ambulant observer can construct a model of the environment from the geometrical structure of the visual flow. In Kybernetik, G. Hauske and F. Butenandt, eds. (Munich: Oldenberg), pp. 224–247.

Koenderink, J.J., and van Doorn, A.J. (1991). Affine structure from motion. J. Opt. Soc. Am. A *8*, 377–385.

Lagae, L., Maes, H., Raiguel, S., Xiao, D.-K., and Orban, G.A. (1994). Responses of macaque STS neurons to optic flow components: a comparison of areas MT and MST. J. Neurophysiol. *71*, 1597–1626.

Leonards, U., Sunaert, S., Van Hecke, P., and Orban, G.A. (1999). Cortical activations during parallel and serial visual search: a fMRI-study. Invest. Ophthalmol. Vis. Sci. *40*, S777.

Liter, J.C., and Braunstein, M.L. (1998). The relationship of vertical and horizontal velocity gradients in the perception of shape, rotation and rigidity. J. Exp. Psychol. Hum. Percept. Perform. *24*, 1257–1272.

Mountcastle, V.B., Lynch, J.C., Georgopoulos, A., Sakara, H., and Acuna, C. (1975). Posterior parietal cortex in the monkey: command functions for operations within extrapersonal space. J. Neurophysiol. *38*, 871–908.

Orban, G.A., Lagae, L., Verri, A., Raiguel, S., Xiao, D., Maes, H., and Torre, V. (1992). First-order analysis of optical flow in monkey brain. Proc. Natl. Acad. Sci. USA *89*, 2595–2599.

Orban, G.A., Dupont, P., Vogels, R., Bormans, G., and Mortelmans, L. (1997). Human brain activity related to orientation discrimination tasks. Eur. J. Neurosci. *9*, 246–259.

Orban, G.A., Dupont, P., De Bruyn, B., Vandenberghe, R., Rosier, A., and Mortelmans, L. (1998). Human brain activity related to speed discrimination tasks. Exp. Brain Res. *122*, 9–22.

Perotti, V.J., Todd, J.T., and Norman, J.F. (1996). The visual perception of rigid motion from constant flow fields. Percept. Psychophys. *58*, 666–679.

Perotti, V.J., Todd, J.T., Lappin, J.S., and Phillips, F. (1998). The perception of surface curvature from optical motion. Percept. Psychophys. *60*, 377–388.

Petit, L., Clark, V.P., Ingeholm, J., and Haxby, J.V. (1997). Dissociation of saccade-related and pursuit-related activation in human frontal eye fields as revealed by fMRI. J. Neurophysiol. *77*, 3386–3390.

Qian, N., and Andersen, R.A. (1994). Transparent motion perception as detection of unbalanced motion signals. II. Physiology. J. Neurosci. *14*, 7367–7380.

Regan, D., and Beverley, K.I. (1978). Looming detectors in the human visual pathway. Vision Res. *18*, 415–421.

Rizzo, M., Nawrot, M., and Zihl, J. (1995). Motion and shape perception in cerebral akinetopsia. Brain *118*, 1105–1127.

Rogers, B., and Graham, M. (1979). Motion parallax as an independent cue for depth perception. Perception *8*, 125–134.

Saito, H., Yukie, M., Tanaka, K., Hikosaka, K., Fukada, Y., and Iwai, E. (1986). Integration of direction signals of image motion in the superior temporal sulcus of the macaque monkey. J. Neurosci. *6*, 145–157.

Sunaert, S., Van Hecke, P., Marchal, G., and Orban, G.A. (1999). Motion responsive regions of the human brain. Exp. Brain Res. *127*, 355–370.

Todd, J.T. (1982). Visual information about rigid and nonrigid motion:

a geometric analysis. J. Exp. Psychol. Hum. Percept. Perform. *8*, 238–251.

Todd, J.T. (1984). The perception of three-dimensional structure from rigid and nonrigid motion. Percept. Psychophys. *36*, 97–103.

Todd, J.T., and Bressan, P. (1990). The perception of 3-dimensional affine structure from minimal apparent motion sequences. Percept. Psychophys. *48*, 419–430.

Todd, J.T., Akerstrom, R.A., Reichel, F.D., and Hayes, W. (1988). Apparent rotation in 3-dimensional space: effects of temporal, spatial and structural factors. Percept. Psychoph. *43*, 179–188.

Tootell, R.B.H., Reppas, J.B., Kwong, K.K., Malach, R., Born, R.T., Brady, T.J., Rosen, B.R., and Belliveau, J.W. (1995). Functional analysis of human MT and related visual cortical areas using magnetic resonance imaging. J. Neurosci. *15*, 3215–3230.

Tootell, R.B.H., Mendola, J.D., Hadjikhani, N.K., Ledden, P.J., Liu, A.K., Reppas, J.B., Sereno, M.I., and Dale, A.M. (1997). Functional analysis of V3A and related areas in human visual cortex. J. Neurosci. *17*, 7060–7078.

Vaina, L.M., Lemay, M., Bienfang, D.C., Choi, A.Y., and Nakayama, K. (1990). Intact "biological motion" and "structure from motion" perception in a patient with impaired motion mechanisms: a case study. Vis. Neurosci. *5*, 353–369.

Vaina, L.M., Royden, C.S., Bienfang, D.C., Makris, N., and Kennedy, D. (1996). Normal perception of heading in a patient with impaired structure-from-motion. Invest. Ophthalmol. Vis. Sci. *37*, S515.

Van Oostende, S., Sunaert, S., Van Hecke, P., Marchal, G., and Orban, G.A. (1997). The kinetic occipital (KO) region in man: an fMRI study. Cereb. Cortex *7*, 690–701.

Wallach, H., and O'Connell, D.N. (1953). The kinetic depth effect. J. Exp. Psychol. *45*, 205–217.

Watson, J.D.G., Myers, R., Frackowiak, R.S.J., Hajnal, J.V., Woods, R.P., Mazziotta, J.C., Shipp, S., and Zeki, S. (1993). Area V5 of the human brain: evidence from a combined study using positron emission tomography and magnetic resonance imaging. Cereb. Cortex *3*, 79–94.

Worsley, K.J., Marrett, S., Neelin, P., Vandal, A.C., Friston, K.J., and Evans, A.C. (1996). A unified statistical approach for determining significant signals in images of cerebral activation. Hum. Brain Map. *4*, 58–73.

Xiao, D.-K., Marcar, V.L., Raiguel, S.E., and Orban, G.A. (1997). Selectivity of macaque MT/V5 neurons for surface orientation in depth specified by motion. Eur. J. Neurosci. *9*, 956–964.

Zeki, S., Watson, J.D.G., Lueck, C.J., Friston, K.J., Kennard, C., and Frackowiak, R.S.J. (1991). A direct demonstration of functional specialization in human visual cortex. J. Neurosci. *11*, 641–649.